Spin dynamics of cold exciton condensates

O. Kyriienko,[1,2] E. B. Magnusson,[1] and I. A. Shelykh[1,2]

[1]*Science Institute, University of Iceland, Dunhagi-3, IS-107 Reykjavik, Iceland*
[2]*Division of Physics and Applied Physics, Nanyang Technological University 637371, Singapore*

We analyze theoretically the dynamics of degenerate four-component condensates of cold indirect excitons. We account for both linear spin-dependent terms arising from spin-orbit interaction of Rashba and Dresselhaus types and nonlinear terms coming from the exciton-exciton interactions. We show that both terms should affect the dynamics of cold exciton droplets in real space and time and lead to the formation of a four-leaf polarization pattern as well as dips in the bright exciton density profile.

I. INTRODUCTION

Collective phenomena are at the root of many remarkable effects in physics. One of their famous manifestations is Bose-Einstein condensation,[1] which occurs if a system of Bose particles is cooled down beyond the critical temperature T_c, which strongly depends on the properties of the individual particles, in particular their effective mass. For systems of cold atoms, where condensing particles are very heavy, T_c lies in the nano-Kelvin regime, which rules out any possibility of the practical implementation of this phenomenon.

On the other hand, in the field of condensed matter physics various candidates were proposed for the realization of BEC with critical temperatures that are orders of magnitude higher than those of cold atoms.[2] The formation of exciton condensates in bulk semiconductors was theoretically predicted more than 40 years ago,[3] but it appeared to be difficult to realize experimentally. Since then, other solid-state candidates have been proposed for achieving high-temperature BEC, including quantum Hall bilayers,[4] magnons,[5] cavity exciton polaritons,[6–8] and indirect excitons.[9,10] The latter system is the focus of the present paper.

A spatially indirect exciton is a bound state of an electron and a hole localized in coupled parallel two-dimensional (2D) layers (Fig. 1). Electron and hole wave functions show a very small overlap, and consequently indirect excitons have a long lifetime compared to ordinary excitons. They behave like metastable particles, which enables them to cool beyond the temperature of quantum degeneracy.[11,12]

Indirect excitons have been widely studied both experimentally and theoretically in recent years. Superfluid behavior of a system of indirect excitons was predicted by Lozovik and Yudson more than 30 years ago,[13] and subsequent theoretical[14–16] and experimental[17–19] studies have suggested that this should be manifested in a series of remarkable effects, including persistent currents, Josephson-related phenomena, and spontaneous pattern formation in real space.

Surprisingly, most of the works dedicated to indirect excitons have neglected their spin structure. On the other hand, it became clear in recent years that taking into account the spinor nature of the condensing bosons can lead to the emergence of novel effects. For cavity polaritons, accounting for the spin led to the appearance of *spinoptronics*, an optical analog of spintronics.[20,21] It was also shown that the spin dependence of polariton-polariton interactions can lead to the appearance of intriguing nonlinear polarization phenomena in polariton condensates, such as polarization multistability,[22] full paramagnetic screening (also known as the spin Meissner effect),[23] and spin-dependent condensate velocities in the hybrid Bose-Fermi systems.[24] One can assume that the spinor structure of indirect excitons also plays an important role for the ground state and dynamic properties of the system.[25,26]

Recently, the spin textures of indirect exciton gas with a long spontaneous coherence length were studied experimentally.[26,37] Crosses in the linear polarization and four-leaf patterns in the circular polarization were observed. This peculiar behavior demonstrates the presence of spin-conversion terms acting on the four possible spin projections of the indirect exciton. In this article, we present a theory of the cold exciton condensate in which both linear spin orbit interaction terms and the nonlinear exchange interaction term are taken into account. It allows us to describe various spin textures and to show the qualitative influence of the different terms.

II. THE MODEL

The spin of an indirect exciton is inherited from spins of the individual electron and heavy hole forming it. The possible spin projections of the electron's spin on the structure growth axis (z axis) are $\pm 1/2$, while possible spin projections of the heavy hole's spin are $\pm 3/2$. The exciton thus can have four possible spin projections: $S_z = \pm 1, \pm 2$ [Fig. 2(a)]. The bright states with $S_z = \pm 1$ can be created by external right or left circular polarized light, while optical creation of the states with $S_z = \pm 2$ is prohibited by selection rules. However, these states, known as *dark states*, cannot be excluded from consideration, as they can appear due to the presence of spin-orbit interaction (SOI) of Rashba or Dresselhaus type, or they can be created as a result of a collision of two bright excitons with opposite circular polarizations, as will be discussed below. For direct excitons, the energies of bright and dark states are split off by electron-hole exchange interaction with a characteristic value of tens of microelectronvolts.[27] However, for indirect excitons, where the overlap between the wave functions of the electrons and holes is very small, this splitting can be neglected and
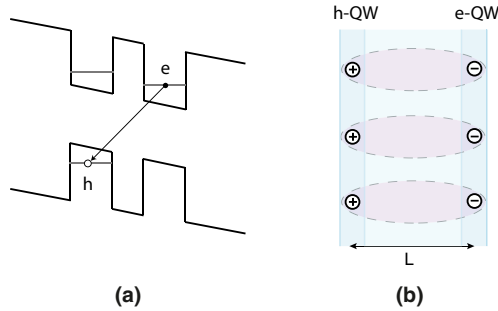
FIG. 1. (Color online) Sketch of the system. (a) Double quantum well heterostructure with applied voltage supports the pairing of an electron in the right QW with a hole in the left QW. (b) Electron-hole bilayer with a schematic picture of a spatially indirect exciton.

bright and dark excitons can be considered to have the same energy.

Below the temperature of the quantum degeneracy, a system of cold indirect excitons can be thus described by a four-component macroscopic wave function $\Psi(\mathbf{r},t) = (\Psi_{+2}(\mathbf{r},t), \Psi_{+1}(\mathbf{r},t), \Psi_{-1}(\mathbf{r},t), \Psi_{-2}(\mathbf{r},t))$, where the subscripts correspond to the z projection of the spin. Its dynamics can be obtained from the following equation:

$$i\hbar\partial_t\Psi_\sigma = \frac{\delta H}{\delta\Psi_\sigma^*}, \tag{1}$$

where H represents the Hamiltonian density of the system accounting for free propagation of particles, SOI, and exciton-exciton interactions, and it can be represented as a sum of single-particle and interaction parts, $H = H_0 + H_{\text{int}}$. Let us consider the terms H_0 and H_{int} separately.

The term H_0 can be calculated as

$$H_0 = \Psi^\dagger(\mathbf{r},t)\hat{\mathbf{T}}\Psi(\mathbf{r},t), \tag{2}$$

where the 4×4 matrix $\hat{\mathbf{T}}$ contains terms corresponding to the kinetic energy and interactions with effective magnetic fields of various types. The latter can be divided into three categories. First, there is SOI acting on the spin of the heavy hole. It scales as a cube of the kinetic momentum[28] and we neglect it in further consideration. As for the SOI acting on electron spin, it can be represented as a sum of the Dresselhaus term $H_D = \beta(\sigma_x\hat{k}_x - \sigma_y\hat{k}_y)$ arising from the lack of inversion symmetry for the crystalline lattices of most common semiconductor materials (GaAs, CdTe, etc.), and the Rashba term $H_R = \alpha(\sigma_x\hat{k}_y - \sigma_y\hat{k}_x)$ appearing due to the structural asymmetry of the QW in the z direction.[29] The coefficients α and β are constants which depend on the material and geometry of the structure, and $\sigma_{x,y}$ are Pauli matrices. For indirect excitons, both Rashba and Dresselhaus terms lead to the transitions $\pm 1 \to \pm 2$ mixing bright and dark exciton states, and the matrix $\hat{\mathbf{T}}$ thus reads

$$\hat{\mathbf{T}} = \begin{pmatrix} \hat{\mathbf{T}}_{12} & 0 \\ 0 & \hat{\mathbf{T}}_{12} \end{pmatrix}, \tag{3}$$

where 2×2 blocks $\hat{\mathbf{T}}_{12}$ can be written in momentum space representation as

$$\hat{\mathbf{T}}_{12}^K = \begin{pmatrix} \hbar^2 K^2/2M & \hat{S}_K \\ \hat{S}_K^* & \hbar^2 K^2/2M \end{pmatrix} \tag{4}$$

with the operator $\hat{S}_K = \chi[\beta(\hat{K}_X + i\hat{K}_Y) + \alpha(\hat{K}_Y + i\hat{K}_X)]$. Here K denotes the center-of-mass momentum of the indirect exciton and $\chi = m_e/M$ is the ratio of effective electron to exciton masses. Regarding the real space representation, one can use the explicit expressions for momentum operators, $\hat{K}_X = -i\partial_X, \hat{K}_Y = -i\partial_Y$. Note that, strictly speaking, when one considers the problem of a single exciton accounting for the effects of the SOI, the latter will affect not only center of mass motion but relative motion as well, producing the slight change of the binding energy of the exciton. This can be accounted for using perturbation theory, and the first nonvanishing correction is of second order (see Appendix A for details of the derivation). We neglect this effect in our further consideration.

Now let us consider the term accounting for exciton-exciton interactions. As indirect excitons are composite bosons,[30,31] they can be divided into four categories, namely the terms corresponding to the direct Coulomb repulsion, exchange of electrons, exchange of holes, and simultaneous exchange of electron and hole (exciton exchange). These processes can be visualized using the interaction diagrams shown in Fig. 2(b).

The corresponding interaction Hamiltonian thus reads

$$\begin{aligned} H_{\text{int}} = {} & \frac{V_{\text{dir}} + V_X + V_e + V_h}{2} \sum_{\sigma=\pm 1\pm 2} |\Psi_\sigma|^4 \\ & + (V_{\text{dir}} + V_X)(|\Psi_{+1}|^2|\Psi_{-1}|^2 + |\Psi_{+2}|^2|\Psi_{-2}|^2) \\ & + (V_{\text{dir}} + V_X + V_e + V_h)(|\Psi_{+1}|^2|\Psi_{+2}|^2 \\ & + |\Psi_{-1}|^2|\Psi_{-2}|^2 + |\Psi_{+1}|^2|\Psi_{-2}|^2 + |\Psi_{-1}|^2|\Psi_{+2}|^2) \\ & + (V_e + V_h)(\Psi_{+1}^*\Psi_{-1}^*\Psi_{+2}\Psi_{-2} + \Psi_{+2}^*\Psi_{-2}^*\Psi_{+1}\Psi_{-1}), \end{aligned} \tag{5}$$

where V_{dir}, V_X, V_e, and V_h denote direct dipole-dipole repulsion, whole exciton exchange, electron exchange, and hole exchange Coulomb interaction, respectively. Since we are interested in the behavior of a weakly depleted Bose-Einstein condensate of indirect excitons, the main contribution comes from the processes with zero transferred momentum, and all values of the matrix elements in the above expression are taken for $q = 0$. It is well known that, contrary to the case of conventional excitons, the spin-independent direct interaction of indirect excitons does not vanish for zero exchanged momenta due to the strong dipole-dipole repulsion.[10,25,32] In addition, the processes of electron and hole exchange also have an influence on the dynamics of the system, making it spin-dependent.

The first term of H_{int} corresponds to the first line of interactions in Fig. 2(b) and describes all possible interactions between indirect excitons of the same spin configuration. The second term corresponds to the processes of the direct Coulomb interaction and exciton exchange shown at the second line. The third and fourth lines of interaction diagrams can be combined in the third term of H_{int}. Finally, the fifth line in Fig. 2(b) corresponds to the fourth term of H_{int} and leads
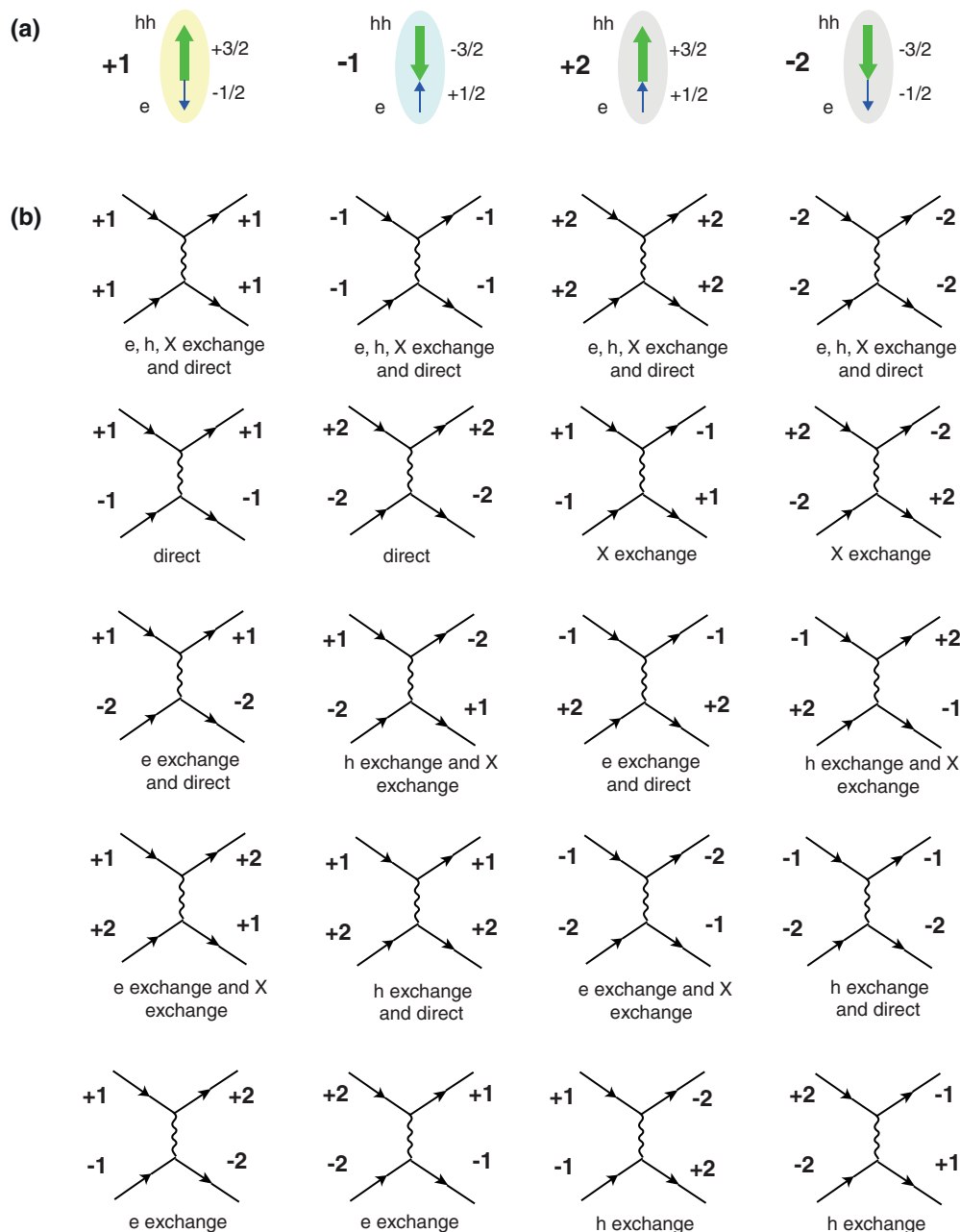
FIG. 2. (Color online) (a) Spin structure of indirect excitons. (b) Feynman diagrams showing different types of possible interactions between two excitons.

to the transition between pairs of bright and dark indirect excitons.

The interaction constants corresponding to all four types of interaction can be estimated in the same fashion as for direct excitons using a narrow QW approximation (see the derivation in Appendix B). The direct Coulomb interaction between indirect excitons is given by

$$V_{\text{dir}} = \frac{e^2 L}{\epsilon \epsilon_0}, \qquad (6)$$

where L is the distance between centers of QWs. The estimation of the electron and hole exchange interaction constant is more cumbersome and requires numerical calculation of an

exchange integral (B17) given in the Appendix B (see also Ref. 33).

For indirect excitons in the long wavelength limit ($q \to 0$), direct and exciton exchange interactions coincide ($V_{\text{dir}} = V_X$) as well as electron and hole exchange ($V_e = V_h$). It should be noted that the electron and hole exchange interaction depends strongly on the distance between the centers of the QWs and changes sign for certain separation, as is shown in Fig. 3. This fact is important for further consideration.

The set of spinor Gross-Pitaevskii equations describing the dynamics of the system and accounting for both linear terms coming from H_0 and nonlinear terms provided by particle-particle interactions of various types can be obtained using

Eqs. (1) and (5) and reads

$$i\hbar\frac{\partial\Psi_{+1}}{\partial t} = \hat{E}\Psi_{+1} - \hat{S}_{12}^*\Psi_{+2} + V_0\Psi_{+1}|\Psi_{+1}|^2 + (V_0-W)\Psi_{+1}|\Psi_{-1}|^2 + V_0\Psi_{+1}(|\Psi_{-2}|^2+|\Psi_{+2}|^2) + W\Psi_{-1}^*\Psi_{+2}\Psi_{-2}, \quad (7)$$

$$i\hbar\frac{\partial\Psi_{-1}}{\partial t} = \hat{E}\Psi_{-1} + \hat{S}_{12}\Psi_{-2} + V_0\Psi_{-1}|\Psi_{-1}|^2 + (V_0-W)\Psi_{-1}|\Psi_{+1}|^2 + V_0\Psi_{-1}(|\Psi_{+2}|^2+|\Psi_{-2}|^2) + W\Psi_{+1}^*\Psi_{+2}\Psi_{-2}, \quad (8)$$

$$i\hbar\frac{\partial\Psi_{+2}}{\partial t} = \hat{E}\Psi_{+2} + \hat{S}_{12}\Psi_{+1} + V_0\Psi_{+2}|\Psi_{+2}|^2 + (V_0-W)\Psi_{+2}|\Psi_{-2}|^2 + V_0\Psi_{+2}(|\Psi_{-1}|^2+|\Psi_{+1}|^2) + W\Psi_{-2}^*\Psi_{+1}\Psi_{-1}, \quad (9)$$

$$i\hbar\frac{\partial\Psi_{-2}}{\partial t} = \hat{E}\Psi_{-2} - \hat{S}_{12}^*\Psi_{-1} + V_0\Psi_{-2}|\Psi_{-2}|^2 + (V_0-W)\Psi_{-2}|\Psi_{+2}|^2 + V_0\Psi_{-2}(|\Psi_{+1}|^2+|\Psi_{-1}|^2) + W\Psi_{+2}^*\Psi_{+1}\Psi_{-1}, \quad (10)$$

where $V_0 = V_{\mathrm{dir}} + V_X + V_e + V_h$, $W = V_e + V_h$, and we defined the kinetic energy operator $\hat{E} = -\hbar^2\nabla^2/2M$. The real space SOI operator reads $\hat{S}_{12} = \chi[\beta(\hat{\partial}_Y - i\hat{\partial}_X) + \alpha(\hat{\partial}_X - i\hat{\partial}_Y)]$. Due to the symmetry between electron and hole exchange at $q = 0$, the set of the equations we consider contains only two independent interaction parameters: V_0, W. This differs from the case considered in Ref. 25, where this symmetry was not accounted for, and five parameters were used for a description of the interactions in the system. In a realistic system, not all of these parameters will be independent.

III. SPECTRUM OF ELEMENTARY EXCITATIONS

The calculation of the spectrum of elementary excitations in the system can be done using the linearization of spinor Gross-Pitaevskii equations (7)–(10) with respect to small perturbation around the ground state. The spin configuration of the ground state of the condensate can be found by minimization of its free energy,

$$F(\Psi_{+1},\Psi_{-1},\Psi_{+2},\Psi_{-2},\mu) = H - \mu f(\Psi_{+1},\Psi_{-1},\Psi_{+2},\Psi_{-2}), \quad (11)$$

where μ denotes the chemical potential of the condensate and $f(\Psi_{+1},\Psi_{-1},\Psi_{+2},\Psi_{-2}) = |\Psi_{+1}|^2 + |\Psi_{-1}|^2 + |\Psi_{+2}|^2 + |\Psi_{-2}|^2$. The condition $f(\Psi_{+1},\Psi_{-1},\Psi_{+2},\Psi_{-2}) = n$, where n is a total concentration, gives an additional equation for the determination of μ.
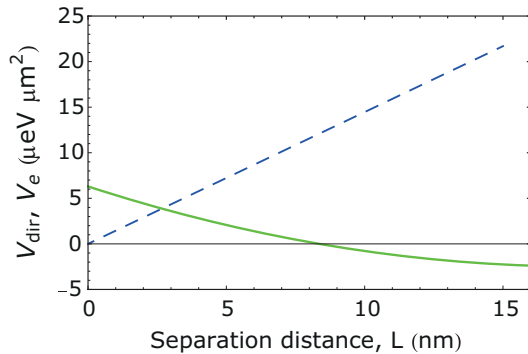

FIG. 3. (Color online) Electron direct (blue dashed line) and exchange (green solid line) interaction for indirect excitons as a function of separation distance between quantum wells L. The sign of the exchange matrix element changes at a certain separation distance. We consider the case of the GaAs/AlGaAs/GaAs heterostructure in the narrow QW limit.

Let us investigate the generic Hamiltonian $H = H_0 + H_{\mathrm{int}}$ more precisely. Its first part H_0 consists of kinetic energy and spin-orbit coupling terms. Both of them depend on the velocity of the particles and can usually be disregarded when considering the ground state, where the interaction Hamiltonian (5) plays a major role. Nevertheless, we will later show that accounting for SOI leads to qualitative changes of the ground state.

The symmetry of H_{int} with respect to the interactions between components results in a nontrivial ground state solution. Let us consider four particular cases of homogeneous condensates:

(i) $|\Psi_{+1}^0| = \sqrt{n}$, $\Psi_{-1,\pm2}^0 = 0$ or $|\Psi_{-1}^0| = \sqrt{n}$, $\Psi_{+1,\pm2}^0 = 0$ or $|\Psi_{+2}^0| = \sqrt{n}$, $\Psi_{-2,\pm1}^0 = 0$ or $|\Psi_{-2}^0| = \sqrt{n}$, $\Psi_{+2,\pm1}^0 = 0$ (one-component condensate);

(ii) $|\Psi_{+1,-1}^0| = \sqrt{n/2}$, $\Psi_{\pm2}^0 = 0$ or $|\Psi_{+2,-2}^0| = \sqrt{n/2}$, $\Psi_{\pm1}^0 = 0$ ("ii" two-component condensate);

(iii) $|\Psi_{+1,-2}^0| = \sqrt{n/2}$, $\Psi_{-1,+2}^0 = 0$ or $|\Psi_{-1,+2}^0| = \sqrt{n/2}$, $\Psi_{+1,-2}^0 = 0$ ("ij" two-component condensate);

(iv) $|\Psi_{\pm1,\pm2}^0| = \sqrt{n/4}$ (four-component condensate);

where we defined the ground state wave function Ψ_i^0 for each component. For instance, the first case implies the situation where only one spin component is present in the condensate with total density n, while the last case implies an equal distribution of the density between the four spin components.

Looking at the interaction Hamiltonian (5), one can note that the last spin-flip term is important. While all other terms do not depend explicitly on the phase of the condensate wave function, it does. Moreover, it is always possible to make the term $\Psi_{+1}^*\Psi_{-1}^*\Psi_{+2}\Psi_{-2}$ negative by adjusting the relative phases of all four condensates, and thus it always lowers the energy of the ground state independently of the sign of the electron exchange term W. However, the sign of W will still affect the ground state properties since it enters into the V_0 matrix element. Thus, one should consider separately two different situations with negative and positive electron and hole exchange interactions.

For negative $W = V_e + V_h < 0$ (large QWs separations), the free energy of the four condensate states considered above is given by

$$H^{(1)} = (V_{\mathrm{dir}} + V_X + V_e + V_h)\frac{n^2}{2} = \frac{V_0 n^2}{2}, \quad (12)$$

$$H_{ii}^{(2)} = \left(V_{\mathrm{dir}} + V_X + \frac{V_e + V_h}{2}\right)\frac{n^2}{2} = \left(V_0 - \frac{W}{2}\right)\frac{n^2}{2}, \quad (13)$$

$$H_{ij}^{(2)} = (V_{\mathrm{dir}} + V_X + V_e + V_h)\frac{n^2}{2} = \frac{V_0 n^2}{2}, \qquad (14)$$

$$H^{(4)} = (V_{\mathrm{dir}} + V_X + V_e + V_h)\frac{n^2}{2} = \frac{V_0 n^2}{2}, \qquad (15)$$

where we denoted by $H^{(1)}$, $H_{ii}^{(2)}$, $H_{ij}^{(2)}$, and $H^{(4)}$ the free energy of one-component, "ii" two-component, "ij" two-component, and four-component condensates, respectively. One can see that the ground state is seven times degenerate, and configurations of one-component, two-component, and four-component condensates are possible. The chemical potential in this case is equal to $\mu_< = (V_{\mathrm{dir}} + V_X + V_e + V_h)n = V_0 n$. Therefore, the ground state of the system will be chosen by a spontaneous symmetry breaking mechanism. The high level of the degeneracy of the ground states means that the system can demonstrate a large variety of topological excitations (solitons, vortices, and skyrmions). Moreover, in the system one can, in principle, observe the fragmentation of the condensate into domains with different spin structure. The analysis of these interesting effects, however, lies beyond the scope of the present paper.

For positive $W = V_e + V_h > 0$ exchange interaction (small QW separations), the free energy of the system for different types of the condensates yields

$$H^{(1)} = (V_{\mathrm{dir}} + V_X + V_e + V_h)\frac{n^2}{2} = \frac{V_0 n^2}{2}, \qquad (16)$$

$$H_{ii}^{(2)} = \left(V_{\mathrm{dir}} + V_X + \frac{V_e + V_h}{2}\right)\frac{n^2}{2} = \left(V_0 - \frac{W}{2}\right)\frac{n^2}{2}, \qquad (17)$$

$$H_{ij}^{(2)} = (V_{\mathrm{dir}} + V_X + V_e + V_h)\frac{n^2}{2} = \frac{V_0 n^2}{2}, \qquad (18)$$

$$H^{(4)} = \left(V_{\mathrm{dir}} + V_X + \frac{V_e + V_h}{2}\right)\frac{n^2}{2} = \left(V_0 - \frac{W}{2}\right)\frac{n^2}{2}. \qquad (19)$$

In this situation, the ground state is three times degenerate, and either a four-component or a two-component condensate in $+1, -1$ or $+2, -2$ configurations is preferable.

The spectrum of elementary excitations in the system can be calculated using the standard method of linearization of the Gross-Pitaevskii equations (7)–(10) with respect to small perturbation taken in form of a plane wave. For instance, in the four-component condensate case with an equal fraction of each spin state, it is taken in the form $\Psi_i^0 = \sqrt{n/4} + A_i e^{i(\mathbf{kr} - \omega t)} + B_i^* e^{-i(\mathbf{kr} - \omega t)}$.[34] The solution of the system of linear algebraic equations for small amplitudes A_i and B_i gives the dispersion relations of the quasiparticles in the condensate.

First, we consider the case when spin-orbit interaction is absent. For large separation between quantum wells, the exchange interaction is attractive and the chemical potential of the ground state is defined as $\mu_< = V_0 n$. The corresponding spectrum of excitations for interaction constants $V_{\mathrm{dir}} = 19.9 \ \mu\mathrm{eV} \ \mu\mathrm{m}^2$ and $V_e = -1.78 \ \mu\mathrm{eV} \ \mu\mathrm{m}^2$ is plotted in Fig. 4(a). It contains a linear Bogoliubov mode, a gapped quadratic mode, and a double degenerate gapless quadratic mode given by relations

$$\hbar\omega_1^< = \sqrt{E_k(E_k + 2\mu_<)}, \qquad (20)$$

$$\hbar\omega_2^< = E_k + n|W|, \qquad (21)$$

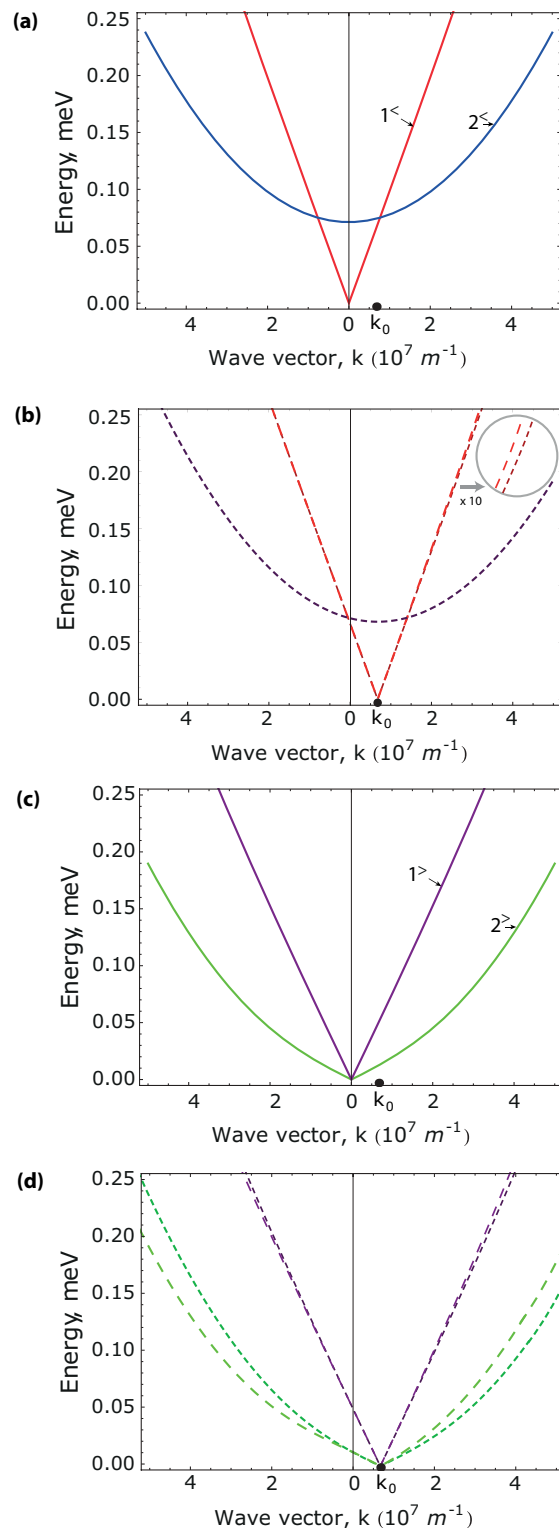$$\hbar\omega_{3,4}^< = E_k, \qquad (22)$$

FIG. 4. (Color online) Quasiparticle modes of a spinor condensate formed by indirect excitons for negative (a),(b) and positive (c),(d) exchange interaction between excitons. The solid lines in the plots (a) and (c) correspond to the dispersions of the quasiparticles without accounting for the spin-orbit interaction, and the numbers indicate the bare modes described by the formulas (20)–(24). Accounting for SOI removes the spin degeneracy and increases the number of modes. Concentration of the particles is taken as $n = 10^9 \ \mathrm{cm}^{-2}$.

where $E_k = \hbar^2 k^2 / 2M$. For the case of small separation between QWs, the exchange matrix element V_e changes sign and becomes repulsive (see Fig. 3). The chemical potential of the ground state is thus defined as $\mu_> = (V_0 - W/2)n$. We plot the spectrum of elementary excitations for $L = 6$ nm separation between wells, where $V_{\mathrm{dir}} = 9.95$ μeV μm^2 and $V_e = 1.24$ μeV μm^2 [Fig. 4(c), solid lines]. The dispersion relations have the form

$$\hbar\omega_{1,3,4}^> = \sqrt{E_k[E_k + 2\mu_>]}, \tag{23}$$

$$\hbar\omega_2^> = \sqrt{E_k(E_k + nW)}, \tag{24}$$

where the modes $\hbar\omega_{1,3,4}$ are now three times degenerate. The obtained spectrum coincides qualitatively with the general dispersion relations given in Ref. 25.

Taking into account the spin-orbit interaction requires including the Rashba and Dresselhaus terms in the Gross-Pitaevskii equations. For the general case of multicomponent gas of cold bosons with spin-orbit coupling, this leads to the unconventional BEC state.[35] One can expect that SOI removes the spin degeneracy and results in the splitting of the modes. Moreover, due to the spin-orbital interaction, a one-component condensate ground state is no longer preferable since the lowest energy state requires the presence of either $(+1,+2)$ or $(-1,-2)$ components. Here we present the numerical calculation of the quasiparticle spectrum, accounting for the isotropic spin-orbit interaction of Rashba type. For the noninteracting case, the dispersion minimum moves to the $k_0 = \pm \frac{M\alpha}{\hbar^2}$ points, which corresponds to the nonzero condensate phase velocity in the ground state (note that group velocity defined as $v_g = \hbar^{-1} dE/dk$ remains equal to zero and the condensate is not moving). The ground state of the condensate in this case acquires the total nonzero phase $e^{i\mathbf{k}_0\mathbf{r}}$, where the orientation of the $\mathbf{k}_0$ vector is defined by the spontaneous symmetry breaking process.

The corresponding renormalization of quasiparticle dispersion now occurs in the vicinity of $\mathbf{k}_0$ points showing a linear spectrum [Figs. 4(b) and 4(d)]. This situation is reminiscent of the renormalization of the bogolon dispersions in the

exciton-polariton condensate, where the role of spin-orbital interaction is played by longitudinal-transverse splitting.[36]

For negative exchange interaction, accounting for Rashba SOI leads to the splitting of degenerate bogolon modes $\hbar\omega_{1,3,4}$, which are linear in the $k = k_0$ region and behave like bare SOI modes far from the k_0 point [Fig. 4(b), red dashed lines]. The gapped mode $\hbar\omega_2$ [Fig. 4(a), red dashed lines] is only slightly renormalized by spin-orbit interaction. One should note that accounting for SOI leads to the ground state formed by an "ij" two-component condensate or a four-component condensate, and rules out the possibility of the formation of a single-component condensate, as was mentioned above.

In the case of positive exchange interaction, both modes $\hbar\omega_{1,3,4}$ and $\hbar\omega_2$ are renormalized in the $k = k_0$ point, while for large values of k they approach the usual Rashba-like dispersion for the upper and lower modes $\varepsilon_\pm = E_k \pm \alpha k$ [Fig. 4(d)]. The ground state in this case corresponds to a four-component condensate only.

A similar situation occurs if only the Dresselhaus interaction term is present in the Hamiltonian. However, if both Rashba and Dresselhaus terms are present, the dispersions of non-renormalized modes are anisotropic. Consequently, states with minimal energy correspond not to a circle, but to two isolated points in the reciprocal space. We leave this case to be a subject for future research.

IV. REAL SPACE AND TIME DYNAMICS

The dynamics of the cold exciton droplet can be studied using the set of four Gross-Pitaevskii equations (7)–(10) formulated in the previous section. In the present article, we consider a GaAs/AlGaAs/GaAs structure with 8 nm/4 nm/8 nm QWs recently studied in Refs. 26 and 37. However, while the only peculiar parameter that affects the behavior of the system is the distance between centers of quantum wells, the qualitative description of spin-conversion terms is general and is applicable for other structures as well, in particular for the case of direct excitons. The initial distribution of the excitons in a droplet is modeled by a 2 μm diameter Gaussian wave packet with
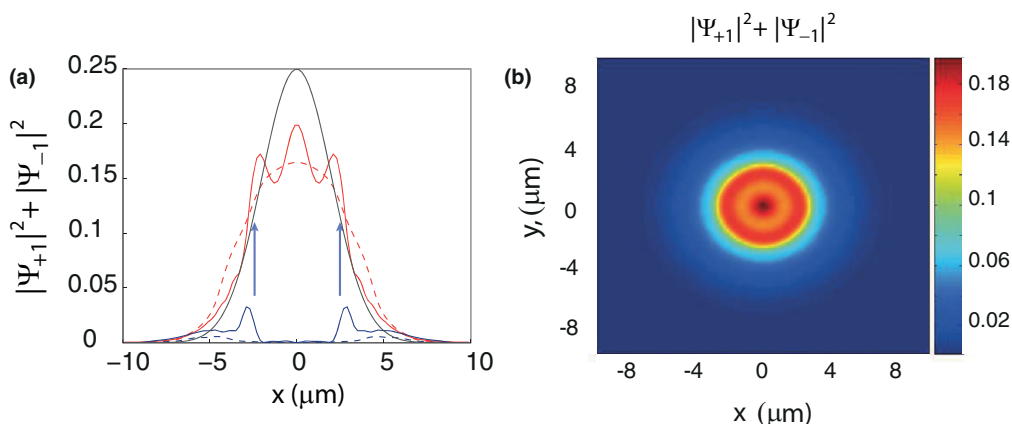

FIG. 5. (Color online) (a) The bright exciton stationary density profile for the linearly polarized two-component ($+1$ and -1) condensate with Dresselhaus SOI present. The spin-orbit interaction constants are taken as $\beta = 3$ μeV μm (red solid line) and $\beta = 1.5$ μeV μm (red dashed line). The gray line represents the initial density profile of the spot (magnitude is reduced by factor of 3), the blue lines corresponds to the concentration of dark exciton states and the arrows indicate the regions of the effective bright-to-dark conversion. (b) The 2D density plot for bright excitons showing the "mexican hat" profile ($\beta = 3$ μeV μm).
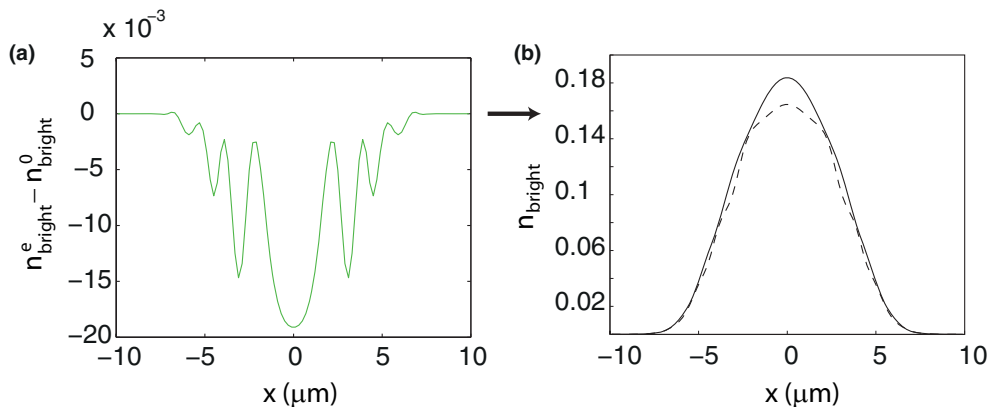
FIG. 6. (Color online) (a) The effect of bright-dark exciton exchange mixing on real space propagation of a cold exciton droplet. The plot shows the difference between distributions of the photoluminescence in cases where bright-dark exciton exchange is present (n_{bright}^e) and absent (n_{bright}^0). (b) The density profile of bright excitons, taking into account the bright-to-dark conversion due to electron and hole exchange (dashed line) and without accounting for the exchange interaction (solid line). The exchange matrix element is equal to $V_e = -V_{dir}/5$, which corresponds to the large separation between QWs.

maximal concentration of the order $n = 10^9$ cm^{-2}. When thermalized and being far from the hot center, the droplets reveal the physics of a cold boson gas, while an additional indirect exciton supply is provided in the central region by external current through the structure.[37] In the present paper, we account for the finite lifetime of the particles ($\tau = 2$ ns) and study the dynamics of the droplets in stationary and nonstationary regimes.

Let us assume that the external optical pump is linearly polarized and both $+1$ and -1 bright exciton states are created. The kinetic terms in the Gross-Pitaevskii equations for Ψ_{+1} and Ψ_{-1} cause the diffusion of the particles from the center of the spot. The strong dipole-dipole interactions lead to the repulsion of particles from the high concentration regions, and this leads to the formation of concentric propagating rings. While the aforementioned terms are present in the case of exciton polariton condensates and they have been widely studied, the additional terms leading to the transitions between bright and dark states are of great importance for the case of indirect excitons. In the following consideration, we describe the effects coming from all terms of this kind separately.

First, if only one type of SOI (Rashba or Dresselhaus) is present, for the cylindrically symmetric pumping spot the distribution of the intensity of the photoluminescence in real space governed by the concentration of bright states remains cylindrically symmetric. The processes of SOI lead to the

conversion of bright states into dark, which can be observed in the bright exciton density plots (Fig. 5). One can note from the form of the SOI operator $\hat{S}_{12}$ that the most efficient conversion of bright states into dark occurs at the points where the density gradient is largest [blue arrows in Fig. 5(a)]. This yields the "mexican hat" profile in the near field distribution of photoluminescence, which depends on SOI strength (solid and dashed lines).

Recently, the appearance of a dip in the center of the photoluminescence (PL) profile was revealed in experiments with indirect excitons in a trap created by strain.[38] Moreover, for high strain, a reappearance of the PL peak in the trap center and the corresponding "mexican hat" profile was observed. The corresponding effects were modeled by accounting for light-hole and heavy-hole (lh-hh) mixing due to strain, which leads to changes in the recombination lifetime of excitons. However, while lh-hh mixing undoubtedly has a strong influence on indirect exciton photoluminescence, one can expect that for high strain, the spin-orbit interaction becomes important when the strain-induced SOI of Rashba and Dresselhaus type appear. Therefore, the effective conversion of bright excitons into dark ones leads to the formation of dips in the PL profile without the change of exciton lifetime. Finally, we can conclude that the interplay of both lh-hh mixing and SOI interaction terms could explain the experimentally observed phenomena in Ref. 38, while an elaborate analysis considering the strain
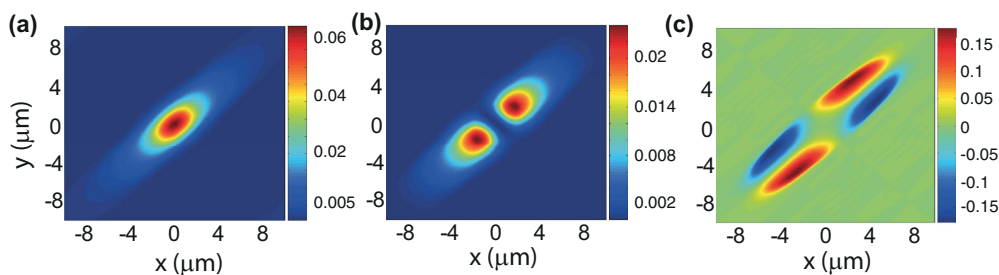

FIG. 7. (Color online) The steady state of a cold exciton droplet with both Rashba and Dresselhaus interactions present ($\beta = 3$ μeV μm, $\alpha = 0.9\beta$). The set of density plots shows the bright exciton (a) and dark exciton (b) density, and the bright circular polarization degree determined as $\wp = (|\Psi_{+1}|^2 - |\Psi_{-1}|^2)/(|\Psi_{+1}|^2 + |\Psi_{-1}|^2)$ (c).
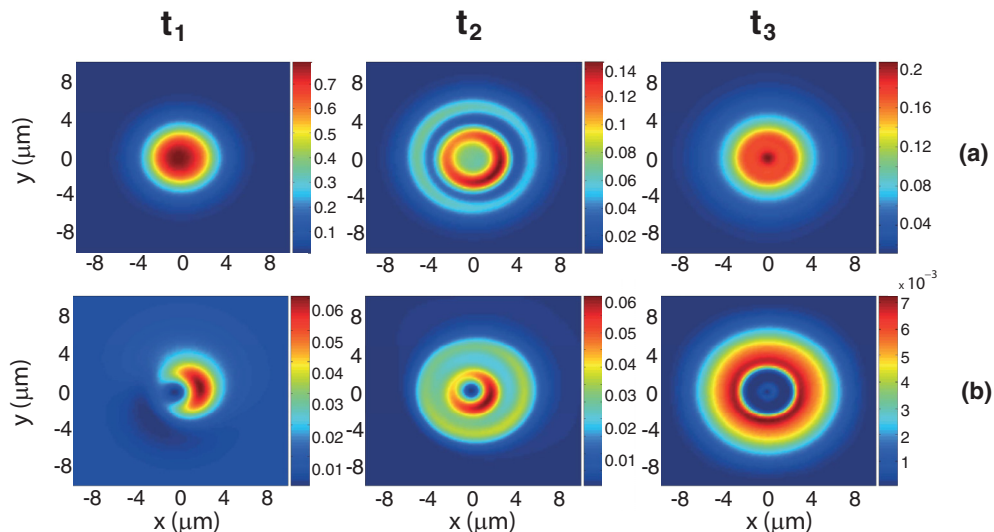
FIG. 8. (Color online) Dynamics of bright (a) and dark (b) components under the circularly polarized initial conditions. The evolution of exciton density reveals the rotation in time of the velocity field for both species, which can be described as resulting from the appearance of the effective magnetic field provided by the interplay between SOI and interactions in the system. The characteristic times for the system are defined by the lifetime of an exciton, $\tau = 2$ ns, and are chosen as $t_1 = 1$ ns, $t_2 = 2$ ns, and $t_3 = 4$ ns.

trap and its effect on lh-hh states is required for a quantitative comparison.

In addition to SOI, another mechanism can lead to bright to dark exciton conversion. This is the electron or hole exchange interaction term leading to the transitions $\{+1,-1\} \longleftrightarrow \{+2,-2\}$. It is described by the last term in the Gross-Pitaevskii equations (7)–(10) with the interaction constant given by $W = V_e + V_h$. In the considered structure, the exchange interaction constant is equal to $V_e = V_h = -1.3 \ \mu\text{eV} \, \mu\text{m}^2$. One can see that the most efficient dark exciton creation process takes place for the highest bright exciton density regions. Together with repulsive interaction dynamics, this leads to the appearance of density modulations in the radial direction connected to the rings of bright exciton concentration. Figure 6(a) shows the difference in the bright exciton density between the case in which the exchange term is present, (n_{bright}^e), and the case in which it is zero, (n_{bright}^0).

One can see that the exchange term leads to the formation of several dips in the bright exciton density and causes an overall flattening of the density profile. For the high density of trapped indirect excitons, bright-to-dark conversion could play an important role, causing the gap in the center of the photoluminescence profile.[38] However, in the typically studied structures with indirect excitons where exchange interaction is an order of magnitude smaller than the direct interaction, the density modulation is weak and can be expected to be concealed by other factors.

Next, we study the situation in which both Rashba and Dresselhaus SOI terms are present in the Gross-Pitaevskii equations. In this case, the dispersions of noninteracting particles are anisotropic in k space,

$$\varepsilon_{\pm}(\mathbf{k}) = \frac{\hbar^2 k^2}{2m} \pm k\sqrt{\alpha^2 + \beta^2 + 2\alpha\beta \sin(2\theta_{\mathbf{k}})}, \qquad (25)$$

where $\theta_{\mathbf{k}}$ denotes the angle between the wave vector $\mathbf{k}$ and the x axis. This can lead to the breaking of cylindrical symmetry in

the system, as is illustrated in Fig. 7. Here we present the steady state plots of the exciton density and polarization, taking into account the finite lifetime of the particles, which are usually measured in the experiments. The density profile in these plots is governed by the interplay of Rashba and Dresselhaus terms, which makes it nonsymmetric in the radial direction. The corresponding evolution of the circular polarization degree shows a four-leaf pattern formation [Fig. 7(c)]. A similar phenomenon was observed experimentally for spots of cold exciton condensates.[37] One can note that in the case of equal strength of Rashba and Dresselhaus SOI, the integrated circular polarization is constantly zero. The spin-orbital interaction depends strongly on the material and geometry of the sample. For the particular 8 nm/4 nm/8 nm GaAs/AlGaAs heterostructure, the constant of Dresselhaus SOI can be estimated as $\beta = 3 \ \mu\text{eV} \, \mu\text{m}$, while the Rashba constant can be tuned in a wide range by the external gate voltage V_g.[29,39,40]

Finally, we consider the case of a circularly polarized condensate where only one component is pumped. In this case, the symmetry between $+1 \rightarrow +2$ and $-1 \rightarrow -2$ conversion is removed, and this leads to the appearance of an effective magnetic field in the z direction acting on bright and dark components and arising from spin-dependent exciton-exciton interactions. Its interplay with SOI of Rashba and Dresslhaus types leads to the rotation of the densities of bright and dark components in real space and time, as is shown in Fig. 8. However, going to the stationary regime, the density profile coincides with the situation for a linear pump (t_3 in Fig. 8).

V. CONCLUSIONS

In conclusion, we analyzed the ground state properties and spin dynamics in the system of cold indirect excitons, accounting for Rashba and Dresselhaus SOI and spin-dependent exciton-exciton interactions. We demonstrated that the ground state of cold exciton gas is highly degenerate, and we

calculated the dispersions of the Bogoliubov excitations in the system. It was shown that accounting for spin structure qualitatively changes the dynamics of the exciton droplets in real space and can lead to the formation of rings and "mexican hat" structures in spatial distribution of near field photoluminescence provided by bright excitons. For the case of both the present Rashba and Dresselhaus terms, we have shown four-leave pattern formation for the distribution of circular polarization in real space.

APPENDIX A: SPIN-ORBIT INTERACTION FOR INDIRECT EXCITON

We consider the indirect exciton–composite boson consisting of an electron and a hole in separated QWs which are bounded with attractive Coulomb interaction. The generic Hamiltonian of an indirect exciton taking into account SOI for the electron (for instance of Rashba type) can be written as

$$\hat{H} = \hat{H}_0 + V_{\text{int}}, \tag{A1}$$

where $V_{\text{int}} = -e^2/4\pi\epsilon\epsilon_0\sqrt{L^2 + |\mathbf{r}_e - \mathbf{r}_h|^2}$ denotes the interaction between an electron and a hole. The kinetic part of the Hamiltonian now includes the SOI term for an electron and can be represented as a 4×4 matrix,

$$\hat{\mathbf{T}} = \begin{pmatrix} \hat{\mathbf{T}}_0 & 0 \\ 0 & \hat{\mathbf{T}}_0 \end{pmatrix}, \tag{A2}$$

where 2×2 blocks $\hat{\mathbf{T}}_0$ read

$$\hat{\mathbf{T}}_0 = \begin{pmatrix} -\frac{\hbar^2}{2m_e}\nabla_e^2 - \frac{\hbar^2}{2m_h}\nabla_h^2 & \alpha(-\partial_x^e + i\partial_y^e) \\ \alpha(\partial_x^e + i\partial_y^e) & -\frac{\hbar^2}{2m_e}\nabla_e^2 - \frac{\hbar^2}{2m_h}\nabla_h^2 \end{pmatrix}, \tag{A3}$$

with m_e and m_h being electron and hole mass, respectively, and we denoted the operators acting on the electron and the hole by the indices e and h. The operator $\hat{\mathbf{T}}$ acts on the spinor wave function $\Psi = (\Psi_{++}, \Psi_{-+}, \Psi_{+-}, \Psi_{--})$, where indices for each component Ψ_{ii} describe the sign of spin projection on the z axis for an electron and a hole. Therefore, nondiagonal terms of matrix $\hat{\mathbf{T}}_0$ couple Ψ_{++} and Ψ_{-+} components and are responsible for the spin-flip transitions between bright and dark excitonic states $\pm 1 \to \pm 2$. For the exciton, this results in bright-to-dark state conversion. The operator $\hat{\mathbf{T}}_0$ can be rewritten in an exciton center-of-mass coordinate frame using transformations,

$$\mathbf{R} = \chi\mathbf{r}_e + (1-\chi)\mathbf{r}_h, \quad \mathbf{r} = \mathbf{r}_e - \mathbf{r}_h,$$

where $\chi = m_e/(m_e + m_h)$ is the electron to exciton mass ratio. Thus, the expression (A3) reads

$$\hat{\mathbf{T}}_0 = \begin{pmatrix} -\frac{\hbar^2}{2M}\nabla_{\mathbf{R}}^2 - \frac{\hbar^2}{2\mu}\nabla_{\mathbf{r}}^2 & \alpha(-\chi\partial_X - \partial_x + i\chi\partial_Y + i\partial_y) \\ \alpha(\chi\partial_X + \partial_x + i\chi\partial_Y + i\partial_y) & -\frac{\hbar^2}{2M}\nabla_{\mathbf{R}}^2 - \frac{\hbar^2}{2\mu}\nabla_{\mathbf{r}}^2 \end{pmatrix}, \tag{A4}$$

with $M = m_e + m_h$ being the exciton mass and $\mu = m_e m_h/M$ being the reduced mass. For simplicity, let us account only for the first matrix $\hat{\mathbf{T}}_0$ acting on the first pair of states Ψ_{++} and Ψ_{-+}. Direct multiplication yields

$$-\frac{\hbar^2}{2M}\nabla_{\mathbf{R}}^2\Psi_{++}(\mathbf{R},\mathbf{r}) + \chi\alpha(-\partial_X + i\partial_Y)\Psi_{-+}(\mathbf{R},\mathbf{r}) + \left[-\frac{\hbar^2}{2\mu}\nabla_{\mathbf{r}}^2 + V(\mathbf{r})\right]\Psi_{++}(\mathbf{R},\mathbf{r}) + \alpha(-\partial_x + i\partial_y)\Psi_{-+}(\mathbf{R},\mathbf{r}) = E\Psi_{++}(\mathbf{R},\mathbf{r}),$$

$$-\frac{\hbar^2}{2M}\nabla_{\mathbf{R}}^2\Psi_{-+}(\mathbf{R},\mathbf{r}) + \chi\alpha(\partial_X + i\partial_Y)\Psi_{++}(\mathbf{R},\mathbf{r}) + \left[-\frac{\hbar^2}{2\mu}\nabla_{\mathbf{r}}^2 + V(\mathbf{r})\right]\Psi_{-+}(\mathbf{R},\mathbf{r}) + \alpha(\partial_x + i\partial_y)\Psi_{++}(\mathbf{R},\mathbf{r}) = E\Psi_{-+}(\mathbf{R},\mathbf{r}).$$

Substituting the wave functions in the plane wave form $\Psi_{++}(\mathbf{R},\mathbf{r}) = e^{i\mathbf{K}\mathbf{R}}\phi_{++}(\mathbf{r})$ and $\Psi_{-+}(\mathbf{R},\mathbf{r}) = e^{i\mathbf{K}\mathbf{R}}\phi_{-+}(\mathbf{r})$, one can see that the Rashba SOI affects the center-of-mass motion of the indirect exciton. Thereby, taking into account the spin-orbit interaction for an electron leads to the appearance of SOI acting on the indirect exciton reduced by a factor $\chi = m_e/M$, denoting the electron-exciton mass ratio. The influence of SOI on relative electron-hole motion can be studied within perturbation theory, and one can show that for the 1s state of an exciton, the first-order correction is zero. Therefore, in the first-order approximation, one can neglect relative motion terms. This allows one to rewrite Eq. (A4) in the form used in the article given by Eq. (4).

In addition to the influence on the single exciton properties, the spin orbit interaction affects the interexciton Coulomb interaction. While in the case of a direct exciton the treatment becomes trickier, for indirect excitons the main contribution comes from dipole-dipole interaction. This allows one to neglect SOI effects for interaction terms of excitons.

APPENDIX B: INTERACTION MATRIX ELEMENTS FOR INDIRECT EXCITONS

The problem of calculating the indirect exciton interaction constant is reminiscent of the same problem for direct excitons. However, one should consider the fact that in the former case, electron and hole layers are separated by a certain distance, and the wave functions of the indirect exciton are modified. The indirect exciton interaction matrix elements were calculated in Ref. 32. However, in the following calculations, we will follow the approach used in Ref. 41 for direct excitons to write integrals in a similar form. As was stated before, spin-dependent exciton interactions are based on four types of

Feynman diagrams: direct interaction, exciton exchange, electron exchange, and hole exchange. These interactions can be written in the general form

$$V_{\text{dir}}(\mathbf{Q},\mathbf{Q}',\mathbf{q}) = \int d^2\mathbf{r_e}d^2\mathbf{r_h}d^2\mathbf{r_{e'}}d^2\mathbf{r_{h'}}\Psi_{\mathbf{Q}}^*(\mathbf{r_e},\mathbf{r_h})\Psi_{\mathbf{Q}'}^*(\mathbf{r_{e'}},\mathbf{r_{h'}})V_I(\mathbf{r_e},\mathbf{r_h},\mathbf{r_{e'}},\mathbf{r_{h'}})\Psi_{\mathbf{Q}+\mathbf{q}}(\mathbf{r_e},\mathbf{r_h})\Psi_{\mathbf{Q}'-\mathbf{q}}(\mathbf{r_{e'}},\mathbf{r_{h'}}), \tag{B1}$$

$$V_X^{\text{exch}}(\mathbf{Q},\mathbf{Q}',\mathbf{q}) = \int d^2\mathbf{r_e}d^2\mathbf{r_h}d^2\mathbf{r_{e'}}d^2\mathbf{r_{h'}}\Psi_{\mathbf{Q}}^*(\mathbf{r_e},\mathbf{r_h})\Psi_{\mathbf{Q}'}^*(\mathbf{r_{e'}},\mathbf{r_{h'}})V_I(\mathbf{r_e},\mathbf{r_h},\mathbf{r_{e'}},\mathbf{r_{h'}})\Psi_{\mathbf{Q}+\mathbf{q}}(\mathbf{r_{e'}},\mathbf{r_{h'}})\Psi_{\mathbf{Q}'-\mathbf{q}}(\mathbf{r_e},\mathbf{r_h}), \tag{B2}$$

$$V_e^{\text{exch}}(\mathbf{Q},\mathbf{Q}',\mathbf{q}) = -\int d^2\mathbf{r_e}d^2\mathbf{r_h}d^2\mathbf{r_{e'}}d^2\mathbf{r_{h'}}\Psi_{\mathbf{Q}}^*(\mathbf{r_e},\mathbf{r_h})\Psi_{\mathbf{Q}'}^*(\mathbf{r_{e'}},\mathbf{r_{h'}})V_I(\mathbf{r_e},\mathbf{r_h},\mathbf{r_{e'}},\mathbf{r_{h'}})\Psi_{\mathbf{Q}+\mathbf{q}}(\mathbf{r_{e'}},\mathbf{r_h})\Psi_{\mathbf{Q}'-\mathbf{q}}(\mathbf{r_e},\mathbf{r_{h'}}), \tag{B3}$$

$$V_h^{\text{exch}}(\mathbf{Q},\mathbf{Q}',\mathbf{q}) = -\int d^2\mathbf{r_e}d^2\mathbf{r_h}d^2\mathbf{r_{e'}}d^2\mathbf{r_{h'}}\Psi_{\mathbf{Q}}^*(\mathbf{r_e},\mathbf{r_h})\Psi_{\mathbf{Q}'}^*(\mathbf{r_{e'}},\mathbf{r_{h'}})V_I(\mathbf{r_e},\mathbf{r_h},\mathbf{r_{e'}},\mathbf{r_{h'}})\Psi_{\mathbf{Q}+\mathbf{q}}(\mathbf{r_e},\mathbf{r_{h'}})\Psi_{\mathbf{Q}'-\mathbf{q}}(\mathbf{r_{e'}},\mathbf{r_h}), \tag{B4}$$

where the Coulomb interaction between the electrons and holes of different excitons is

$$V_I(\mathbf{r_e},\mathbf{r_h},\mathbf{r_{e'}},\mathbf{r_{h'}}) = V(|\mathbf{r_e}-\mathbf{r_{e'}}|) + V(|\mathbf{r_h}-\mathbf{r_{h'}}|) - V(|\mathbf{r_e}-\mathbf{r_{h'}}|) - V(|\mathbf{r_{e'}}-\mathbf{r_h}|),$$

where the minus sign for the last two terms indicates an attractive interaction between an electron and a hole.

The Coulomb interaction for indirect excitons can be written as

$$V_I(\mathbf{r_e},\mathbf{r_h},\mathbf{r_{e'}},\mathbf{r_{h'}}) = \frac{e^2}{4\pi\epsilon\epsilon_0}\left[\frac{1}{|\mathbf{r_e}-\mathbf{r_{e'}}|} + \frac{1}{|\mathbf{r_h}-\mathbf{r_{h'}}|} - \frac{1}{\sqrt{(\mathbf{r_e}-\mathbf{r_{h'}})^2+L^2}} - \frac{1}{\sqrt{(\mathbf{r_h}-\mathbf{r_{e'}})^2+L^2}}\right],$$

where L is a separation distance between centers of coupled QWs, and we used a narrow QW approximation. In the main text of the article, we omit superscript indices "exch" for the sake of brevity.

There are several possible ways to construct the wave function of an indirect exciton. As in the usual case of direct excitons, we consider the 2D motion of a bounded electron-hole pair but with fixed separation in the z direction equal to L. In this case, it is convenient to separate the exciton center of mass motion and the relative motion. The general form of the wave function is

$$f(\mathbf{r}_\parallel,\mathbf{R}_\parallel) = \frac{e^{i\mathbf{K}_\parallel\mathbf{R}_\parallel}}{\sqrt{A}}\phi(\mathbf{r}_\parallel),$$

where new coordinates are $\mathbf{r}_\parallel = \mathbf{r}_\parallel^e - \mathbf{r}_\parallel^h$ describing relative motion and $\mathbf{R}_\parallel = \beta_e\mathbf{r}_\parallel^e + \beta_h\mathbf{r}_\parallel^h$ for exciton center-of-mass motion. Here $\beta_e = m_e/(m_e+m_h)$, $\beta_h = m_h/(m_e+m_h)$, and A denotes the area of the sample. While the center of mass motion is described by the plane wave function, the relative motion part of the wave function $\phi(\mathbf{r}_\parallel)$ can be represented in several different forms,[33]

$$\phi_1(\mathbf{r}_\parallel) = \sqrt{\frac{2}{\pi}}\frac{1}{a_B}\exp\left(-\frac{|\mathbf{r}_\parallel|}{a_B}\right), \tag{B5}$$

$$\phi_2(\mathbf{r}_\parallel) = \frac{1}{\sqrt{2\pi b(b+r_0)}}\exp\left(-\frac{\sqrt{r_\parallel^2+r_0^2}-r_0}{2b}\right), \tag{B6}$$

where a_B and $2b$ are quantities associated with indirect exciton Bohr radii obtained by the variational procedure, and r_0 is a variational parameter reminiscent of the separation distance between QWs.

1. Direct and exciton exchange interaction of indirect excitons

To calculate the direct dipole-dipole interaction of two indirect excitons, we choose the second representation of the wave function with $\phi(\mathbf{r}_\parallel) = \phi_2(\mathbf{r}_\parallel)$. In the following derivation, we will omit the sign $\parallel$ meaning 2D motion everywhere. Thus, the integral can be written as

$$V_{\text{dir}}(\mathbf{Q},\mathbf{Q}',\mathbf{q}) = \frac{e^2}{4\pi\epsilon\epsilon_0 A^2}\frac{\exp(2r_0/b)}{[2\pi b(b+r_0)]^2}\int d^2\mathbf{r}_e d^2\mathbf{r}_h d^2\mathbf{r}_{e'} d^2\mathbf{r}_{h'}\exp\left(-\frac{\sqrt{(\mathbf{r}_e-\mathbf{r}_h)^2+r_0^2}}{b}\right)\exp\left(-\frac{\sqrt{(\mathbf{r}_{e'}-\mathbf{r}_{h'})^2+r_0^2}}{b}\right)$$

$$\times \exp[-i\mathbf{Q}(\beta_e\mathbf{r}_e+\beta_h\mathbf{r}_h)]\exp[-i\mathbf{Q}'(\beta_e\mathbf{r}_{e'}+\beta_h\mathbf{r}_{h'})]\left[\frac{1}{|\mathbf{r}_e-\mathbf{r}_{e'}|} + \frac{1}{|\mathbf{r}_h-\mathbf{r}_{h'}|} - \frac{1}{\sqrt{(\mathbf{r}_e-\mathbf{r}_{h'})^2+L^2}}\right.$$

$$\left. - \frac{1}{\sqrt{(\mathbf{r}_h-\mathbf{r}_{e'})^2+L^2}}\right]\exp[i(\mathbf{Q}+\mathbf{q})(\beta_e\mathbf{r}_e+\beta_h\mathbf{r}_h)]\exp[i(\mathbf{Q}'-\mathbf{q})(\beta_e\mathbf{r}_{e'}+\beta_h\mathbf{r}_{h'})]. \tag{B7}$$

This integral can be simplified if one introduces center-of-motion coordinates for both indirect excitons: $\mathbf{R} = \beta_e \mathbf{r}_e + \beta_h \mathbf{r}_h$, $\mathbf{R}' = \beta_e \mathbf{r}_{e'} + \beta_h \mathbf{r}_{h'}$, $\boldsymbol{\rho} = \mathbf{r}_e - \mathbf{r}_h$, and $\boldsymbol{\rho}' = \mathbf{r}_{e'} - \mathbf{r}_{h'}$. Then Eq. (B7) yields

$$
V_{\mathrm{dir}}(\mathbf{q}) = \frac{e^2}{4\pi\epsilon\epsilon_0 A^2} \frac{\exp(2r_0/b)}{[2\pi b(b+r_0)]^2} \int d^2\boldsymbol{\rho}\, d^2\boldsymbol{\rho}' d^2\mathbf{R}\, d^2\mathbf{R}' \exp\left(-\frac{\sqrt{\boldsymbol{\rho}^2 + r_0^2}}{b}\right) \exp\left(-\frac{\sqrt{\boldsymbol{\rho}'^2 + r_0^2}}{b}\right) \exp[i\mathbf{q}(\mathbf{R} - \mathbf{R}')]
$$
$$
\times \left[\frac{1}{|\beta_h(\boldsymbol{\rho} - \boldsymbol{\rho}') + \mathbf{R} - \mathbf{R}'|} + \frac{1}{|-\beta_e(\boldsymbol{\rho} - \boldsymbol{\rho}') + \mathbf{R} - \mathbf{R}'|} - \frac{1}{\sqrt{(\beta_h\boldsymbol{\rho} + \beta_e\boldsymbol{\rho}' + \mathbf{R} - \mathbf{R}')^2 + L^2}} \right.
$$
$$
\left. - \frac{1}{\sqrt{(-\beta_e\boldsymbol{\rho} - \beta_h\boldsymbol{\rho}' + \mathbf{R} - \mathbf{R}')^2 + L^2}} \right],
\tag{B8}
$$

where one can note that complex exponents with $\mathbf{Q}$ and $\mathbf{Q}'$ cancel each other. It is convenient to use the next substitutions $\boldsymbol{\xi} = \mathbf{R} - \mathbf{R}'$, $\boldsymbol{\sigma} = (\mathbf{R} + \mathbf{R}')/2$. The integral (B8) rewritten with new variables reads

$$
V_{\mathrm{dir}}(\mathbf{q}) = \frac{e^2}{4\pi\epsilon\epsilon_0 A} \frac{\exp(2r_0/b)}{[2\pi b(b+r_0)]^2} \int d^2\boldsymbol{\rho}\, d^2\boldsymbol{\rho}' d^2\boldsymbol{\xi} \exp\left(-\frac{\sqrt{\boldsymbol{\rho}^2 + r_0^2}}{b}\right) \exp\left(-\frac{\sqrt{\boldsymbol{\rho}'^2 + r_0^2}}{b}\right) \exp[i\mathbf{q}\boldsymbol{\xi}]
$$
$$
\times \left[\frac{1}{|\beta_h(\boldsymbol{\rho} - \boldsymbol{\rho}') + \boldsymbol{\xi}|} + \frac{1}{|-\beta_e(\boldsymbol{\rho} - \boldsymbol{\rho}') + \boldsymbol{\xi}|} - \frac{1}{\sqrt{(\beta_h\boldsymbol{\rho} + \beta_e\boldsymbol{\rho}' + \boldsymbol{\xi})^2 + L^2}} - \frac{1}{\sqrt{(-\beta_e\boldsymbol{\rho} - \beta_h\boldsymbol{\rho}' + \boldsymbol{\xi})^2 + L^2}} \right],
\tag{B9}
$$

where the two-dimensional integral over variable $\boldsymbol{\sigma}$ gives the area A. The expression (B9) represents a sum of four integrals for electron-electron, hole-hole, and electron-hole mixed interaction,

$$
V_{\mathrm{dir}} = [\mathcal{I}_{ee'} + \mathcal{I}_{hh'} - \mathcal{I}_{eh'} - \mathcal{I}_{he'}].
\tag{B10}
$$

Let us calculate all integrals separately. The first integral $\mathcal{I}_{ee'}$ yields

$$
\mathcal{I}_{ee'}(\mathbf{q}) = C \int d^2\boldsymbol{\rho}\, d^2\boldsymbol{\rho}' d^2\boldsymbol{\xi} \exp\left(-\frac{\sqrt{\boldsymbol{\rho}^2 + r_0^2}}{b}\right) \exp\left(-\frac{\sqrt{\boldsymbol{\rho}'^2 + r_0^2}}{b}\right) \exp[i\mathbf{q}\boldsymbol{\xi}] \left[\frac{1}{\sqrt{\beta_h^2(\boldsymbol{\rho} - \boldsymbol{\rho}')^2 + \boldsymbol{\xi}^2}} \right]
$$
$$
= C \int d^2\boldsymbol{\rho}\, d^2\boldsymbol{\rho}' \exp\left(-\frac{\sqrt{\boldsymbol{\rho}^2 + r_0^2}}{b}\right) \exp\left(-\frac{\sqrt{\boldsymbol{\rho}'^2 + r_0^2}}{b}\right) \int_0^{+\infty} \frac{\xi d\xi}{\sqrt{a^2 + \xi^2}} \int_0^{2\pi} d\phi \exp(iq\xi\cos\phi)
$$
$$
= 2\pi C \int d^2\boldsymbol{\rho}\, d^2\boldsymbol{\rho}' \exp\left(-\frac{\sqrt{\boldsymbol{\rho}^2 + r_0^2}}{b}\right) \exp\left(-\frac{\sqrt{\boldsymbol{\rho}'^2 + r_0^2}}{b}\right) \int_0^{+\infty} d\xi \frac{\xi J_0(q\xi)}{\sqrt{a^2 + \xi^2}}
$$
$$
= \frac{2\pi}{q} C \int d^2\boldsymbol{\rho}\, d^2\boldsymbol{\rho}' \exp\left(-\frac{\sqrt{\boldsymbol{\rho}^2 + r_0^2}}{b}\right) \exp\left(-\frac{\sqrt{\boldsymbol{\rho}'^2 + r_0^2}}{b}\right) \exp[-\beta_h\mathbf{q}\boldsymbol{\rho}] \exp[\beta_h\mathbf{q}\boldsymbol{\rho}'],
\tag{B11}
$$

where we defined the constant $C = \frac{e^2}{4\pi\epsilon\epsilon_0 A} \frac{\exp(2r_0/b)}{[2\pi b(b+r_0)]^2}$ and made the substitution $a^2 = \beta_h^2(\boldsymbol{\rho} - \boldsymbol{\rho}')^2$. The integrals on $\boldsymbol{\rho}$ and $\boldsymbol{\rho}'$ are identical and can be factorized into $\mathcal{I}_{ee'}(\mathbf{q}) = C\mathcal{I}_\rho^2(\mathbf{q})$, where

$$
\mathcal{I}_\rho(\mathbf{q}) = \int d\rho\rho \exp\left(-\frac{\sqrt{\rho^2 + r_0^2}}{b}\right) \int_0^{2\pi} e^{-\beta_h q\rho\cos\phi} d\phi = 2\pi \int d\rho\rho \exp\left(-\frac{\sqrt{\rho^2 + r_0^2}}{b}\right) J_0(\beta_h q\rho).
\tag{B12}
$$

It is not possible to calculate integral (B12) analytically in the general case, but we are interested in the $q = 0$ limit. Then we can change the variable to $x^2 = \rho^2 + r_0^2$ and integrate by parts,

$$
\mathcal{I}_\rho(\mathbf{q} \to 0) = 2\pi \int_0^{+\infty} d\rho\, \rho \exp\left(-\frac{\sqrt{\rho^2 + r_0^2}}{b}\right) = 2\pi \int_{r_0}^{+\infty} dx\, x e^{-x/b} = 2\pi e^{-r_0/b} b(b + r_0).
$$

Finally, the integral $\mathcal{I}_{ee'}$ reads

$$
\mathcal{I}_{ee'}^{\mathbf{q} \to 0} = \frac{e^2}{4\pi\epsilon\epsilon_0 A} \frac{\exp(2r_0/b)}{[2\pi b(b+r_0)]^2} \frac{2\pi}{q} [2\pi e^{-r_0/b} b(b + r_0)]^2 = \frac{e^2}{2\pi\epsilon\epsilon_0 A q}.
$$

One can see that the expression for the integral $\mathcal{I}_{hh'}$ coincides with $\mathcal{I}_{ee'}$ with the substitution $\beta_h \to \beta_e$. Therefore, in the $q \to 0$ limit they are equal to $\mathcal{I}_{hh'} = e^2/2\pi\epsilon\epsilon_0 Aq$.

Now let us calculate the second type of integrals responsible for the electron-hole attractive interaction,

$$\mathcal{I}_{eh'}(\mathbf{q}) = C \int d^2\boldsymbol{\rho} d^2\boldsymbol{\rho}' d^2\boldsymbol{\xi} \exp\left(-\frac{\sqrt{\boldsymbol{\rho}^2 + r_0^2}}{b}\right) \exp\left(-\frac{\sqrt{\boldsymbol{\rho}'^2 + r_0^2}}{b}\right) \exp[i\mathbf{q}\boldsymbol{\xi}]\left[\frac{1}{\sqrt{(\beta_h\boldsymbol{\rho} + \beta_e\boldsymbol{\rho}' + \boldsymbol{\xi})^2 + L^2}}\right],$$

and performing the substitution $\boldsymbol{\chi} = \beta_h\boldsymbol{\rho} + \beta_e\boldsymbol{\rho}' + \boldsymbol{\xi}$, we can write

$$\mathcal{I}_{eh'}(\mathbf{q}) = C \int d^2\boldsymbol{\rho}\, d^2\boldsymbol{\rho}' d^2\boldsymbol{\chi} \exp\left(-\frac{\sqrt{\boldsymbol{\rho}^2 + r_0^2}}{b}\right) \exp\left(-\frac{\sqrt{\boldsymbol{\rho}'^2 + r_0^2}}{b}\right) \exp[-i\mathbf{q}\boldsymbol{\chi}] \exp[-i\beta_h\mathbf{q}\boldsymbol{\rho}] \exp[-i\beta_e\mathbf{q}\boldsymbol{\rho}']\left[\frac{1}{\sqrt{\boldsymbol{\chi}^2 + L^2}}\right]$$

$$= C \int d^2\boldsymbol{\rho} d^2\boldsymbol{\rho}' \exp\left(-\frac{\sqrt{\boldsymbol{\rho}^2 + r_0^2}}{b}\right) \exp\left(-\frac{\sqrt{\boldsymbol{\rho}'^2 + r_0^2}}{b}\right) \exp[-i\beta_h\mathbf{q}\boldsymbol{\rho}] \exp[-i\beta_e\mathbf{q}\boldsymbol{\rho}'] \int_0^{+\infty} d\chi \frac{\chi}{\sqrt{\chi^2 + L^2}} \int_0^{2\pi} d\phi\, e^{iq\chi\cos\phi}$$

$$= C \frac{2\pi e^{-qL}}{q} \int d^2\boldsymbol{\rho}\, d^2\boldsymbol{\rho}' \exp\left(-\frac{\sqrt{\boldsymbol{\rho}^2 + r_0^2}}{b}\right) \exp\left(-\frac{\sqrt{\boldsymbol{\rho}'^2 + r_0^2}}{b}\right) \exp[-i\beta_h\mathbf{q}\boldsymbol{\rho}] \exp[-i\beta_e\mathbf{q}\boldsymbol{\rho}']. \tag{B13}$$

The same factorization can be done as in the integral (B11), and expression (B13) yields

$$\mathcal{I}_{eh'}(\mathbf{q} \to 0) = \frac{e^2}{2\pi\epsilon\epsilon_0 A} \frac{e^{-qL}}{q}. \tag{B14}$$

One can check that the same expression is valid for $\mathcal{I}_{he'}(\mathbf{q} \to 0)$. Finally, the sum of four integrals yields

$$V_{\text{dir}}^{q\to 0} = \lim_{q\to 0} \frac{e^2}{\epsilon\epsilon_0 A} \frac{(1 - e^{-qL})}{q} = \frac{e^2}{\epsilon\epsilon_0 A} L. \tag{B15}$$

A similar result was obtained using another approach by the authors of Ref. 32.

The exciton exchange interaction V_X^{exch} can be written in the same way as direct interaction from the general form (B2),

$$V_X^{\text{exch}}(\mathbf{Q},\mathbf{Q}',\mathbf{q}) = \frac{e^2}{4\pi\epsilon\epsilon_0 A^2} \frac{\exp(2r_0/b)}{[2\pi b(b + r_0)]^2} \int d^2\mathbf{r}_e d^2\mathbf{r}_h d^2\mathbf{r}_{e'} d^2\mathbf{r}_{h'} \exp\left(-\frac{\sqrt{(\mathbf{r}_e - \mathbf{r}_h)^2 + r_0^2}}{b}\right) \exp\left(-\frac{\sqrt{(\mathbf{r}_{e'} - \mathbf{r}_{h'})^2 + r_0^2}}{b}\right)$$

$$\times \exp[-i\mathbf{Q}(\beta_e\mathbf{r}_e + \beta_h\mathbf{r}_h)] \exp[-i\mathbf{Q}'(\beta_e\mathbf{r}_{e'} + \beta_h\mathbf{r}_{h'})]\left[\frac{1}{|\mathbf{r}_e - \mathbf{r}_{e'}|} + \frac{1}{|\mathbf{r}_h - \mathbf{r}_{h'}|} - \frac{1}{\sqrt{(\mathbf{r_e} - \mathbf{r_{h'}})^2 + L^2}}\right.$$

$$\left. - \frac{1}{\sqrt{(\mathbf{r_h} - \mathbf{r_{e'}})^2 + L^2}}\right] \exp[i(\mathbf{Q} + \mathbf{q})(\beta_e\mathbf{r}_{e'} + \beta_h\mathbf{r}_{h'})] \exp[i(\mathbf{Q}' - \mathbf{q})(\beta_e\mathbf{r}_e + \beta_h\mathbf{r}_h)]$$

$$= \frac{e^2}{4\pi\epsilon\epsilon_0 A^2} \frac{\exp(2r_0/b)}{[2\pi b(b + r_0)]^2} \int d^2\boldsymbol{\rho} d^2\boldsymbol{\rho}' d^2\mathbf{R} d^2\mathbf{R}' \exp\left(-\frac{\sqrt{\boldsymbol{\rho}^2 + r_0^2}}{b}\right) \exp\left(-\frac{\sqrt{\boldsymbol{\rho}'^2 + r_0^2}}{b}\right) \exp[-i\Delta\mathbf{Q}(\mathbf{R} - \mathbf{R}')]$$

$$\times \exp[-i\mathbf{q}(\mathbf{R} - \mathbf{R}')]\left[\frac{1}{|\beta_h(\boldsymbol{\rho} - \boldsymbol{\rho}') + \mathbf{R} - \mathbf{R}'|} + \frac{1}{|-\beta_e(\boldsymbol{\rho} - \boldsymbol{\rho}') + \mathbf{R} - \mathbf{R}'|}\right.$$

$$\left. - \frac{1}{\sqrt{(\beta_h\boldsymbol{\rho} + \beta_e\boldsymbol{\rho}' + \mathbf{R} - \mathbf{R}')^2 + L^2}} - \frac{1}{\sqrt{(-\beta_e\boldsymbol{\rho} - \beta_h\boldsymbol{\rho}' + \mathbf{R} - \mathbf{R}')^2 + L^2}}\right],$$

where we defined exchanged momentum between electrons as $\Delta\mathbf{Q} = \mathbf{Q} - \mathbf{Q}'$. One can see that for small exchanged momentum between the excitons, which is true for weakly interacting exciton gas, the expression for V_X^{exch} coincides with V_{dir} for $q \to 0$.

2. Electron and hole exchange interaction of indirect excitons

The general form of electron exchange interaction for indirect excitons is given by Eq. (B3). For the calculations, it is more convenient to choose the indirect exciton wave function in the form (B5). Thus the exchange interaction matrix element yields

$$
\begin{aligned}
V_e^{\text{exch}}(\mathbf{Q},\mathbf{Q}',\mathbf{q}) = {} & -\frac{e^2}{4\pi\epsilon\epsilon_0 A^2}\frac{4}{\pi^2 a_B^4}\int d^2\mathbf{r_e}d^2\mathbf{r_h}d^2\mathbf{r_{e'}}d^2\mathbf{r_{h'}}\exp\left(-\frac{\sqrt{(\mathbf{r}_e-\mathbf{r}_h)^2+L^2}}{a_B}\right)\exp\left(-\frac{\sqrt{(\mathbf{r}_{e'}-\mathbf{r}_{h'})^2+L^2}}{a_B}\right) \\
& \times \exp\left(-\frac{\sqrt{(\mathbf{r}_{e'}-\mathbf{r}_h)^2+L^2}}{a_B}\right)\exp\left(-\frac{\sqrt{(\mathbf{r}_e-\mathbf{r}_{h'})^2+L^2}}{a_B}\right)\exp[-i\mathbf{Q}(\beta_e\mathbf{r}_e+\beta_h\mathbf{r}_h)]\exp[-i\mathbf{Q}'(\beta_e\mathbf{r}_{e'}+\beta_h\mathbf{r}_{h'})] \\
& \times \exp[i(\mathbf{Q}+\mathbf{q})(\beta_e\mathbf{r}_e+\beta_h\mathbf{r}_h)]\exp[i(\mathbf{Q}'-\mathbf{q})(\beta_e\mathbf{r}_{e'}+\beta_h\mathbf{r}_{h'})] \\
& \times \left[\frac{1}{|\mathbf{r}_e-\mathbf{r}_{e'}|}+\frac{1}{|\mathbf{r}_h-\mathbf{r}_{h'}|}-\frac{1}{\sqrt{(\mathbf{r}_e-\mathbf{r}_{h'})^2+L^2}}-\frac{1}{\sqrt{(\mathbf{r}_h-\mathbf{r}_{e'})^2+L^2}}\right].
\end{aligned}
$$

The exact calculation of the exchange integral is straightforward but tedious. Using the same steps as for direct interaction calculation and performing in the end substitutions $\mathbf{y}_1=(\boldsymbol{\xi}-\beta_e\boldsymbol{\rho}-\beta_h\boldsymbol{\rho}')/a_B$, $\mathbf{y}_2=(\boldsymbol{\xi}+\beta_h\boldsymbol{\rho}+\beta_e\boldsymbol{\rho}')/a_B$, $\mathbf{x}=\boldsymbol{\rho}/a_B$, and $\widetilde{L}=L/a_B$, one gets the final expression of electron exchange interaction,

$$
V_e^{\text{exch}}=-\frac{e^2}{4\pi\epsilon\epsilon_0 A}\left(\frac{2}{\pi}\right)^2 a_B\mathcal{I}_e^{\text{exch}}(\Delta Q,q,\Theta,\beta_e), \tag{B16}
$$

where the exchange integral is given by

$$
\begin{aligned}
\mathcal{I}_e^{\text{exch}}(\Delta Q,q,\Theta,\beta_e) = {} & \int_0^\infty dx\int_0^{2\pi}d\Theta_x\int_0^\infty dy_1\int_0^{2\pi}d\Theta_1\int_0^\infty dy_2\int_0^{2\pi}d\Theta_2\, xy_1y_2\cos[\Delta Qa_B[\beta_e x\cos(\Theta-\Theta_x) \\
& + \beta_e y_1\cos(\Theta-\Theta_1)]+qa_B[-x\cos\Theta_x-\beta_e y_1\cos\Theta_1+(1-\beta_e y_2\cos\Theta_2)]] \\
& \times \exp(-\sqrt{x^2+\widetilde{L}^2})\exp\left(-\sqrt{y_1^2+\widetilde{L}^2}\right)\exp\left(-\sqrt{y_2^2+\widetilde{L}^2}\right) \\
& \times \exp[-\sqrt{(y_2\cos\Theta_2-y_1\cos\Theta_1-x\cos\Theta_x)^2+(y_2\sin\Theta_2-y_1\sin\Theta_1-x\sin\Theta_x)^2+\widetilde{L}^2}] \\
& \times \left[\frac{1}{\sqrt{y_1^2+x^2+2y_1x\cos(\Theta_1-\Theta_x)}}\frac{1}{\sqrt{y_2^2+x^2+2y_2x\cos(\Theta_2-\Theta_x)}}-\frac{1}{\sqrt{y_1^2+\widetilde{L}^2}}-\frac{1}{\sqrt{y_2^2+\widetilde{L}^2}}\right],
\end{aligned}
$$
$$\tag{B17}$$

with Θ being the angle between $\Delta\mathbf{Q}$ and $\mathbf{q}$. We are interested in the case when $\Delta Q=0$ and $q=0$. The calculation of the exchange integral thus requires numerical integration with a multidimensional Monte Carlo algorithm. Moreover, it is obvious that, similar to the case of direct excitons, electron and hole exchange interactions have the same value for $q\to 0$.

[1]L. Pitaevskii and S. Stringari, *Bose-Einstein Condensation* (Oxford University Press, Oxford, 2003); A. Legett, *Quantum Liquids: Bose Condensation and Cooper Pairing in Condensed-Matter Systems* (Oxford University Press, Oxford, 2006).

[2]S. A. Moskalenko and D. W. Snoke, *Bose-Einstein Condensation of Excitons and Biexcitons* (Cambridge University Press, Cambridge, UK, 2000).

[3]L. V. Keldysh and Yu. V. Kopaev, Sov. Phys. Solid State **6**, 2219 (1965) [Sov. Phys. JETP **27**, 521 (1968)].

[4]I. B. Spielman, J. P. Eisenstein, L. N. Pfeiffer, and K. W. West, Phys. Rev. Lett. **87**, 036803 (2001); J. P. Eisenstein and A. H. MacDonald, Nature (London) **432**, 691 (2004).

[5]S. O. Demokritov, V. E. Demidov, O. Dzyapko, G. A. Melkov, A. A. Serga, B. Hillebrands, and A. N. Slavin, Nature (London) **443**, 430 (2006).

[6]J. Kasprzak, M. Richard, S. Kundermann, A. Baas, P. Jeambrun, J. M. J. Keeling, F. M. Marchetti, M. H. Szymanska, R. Andre, J. L. Staehli, V. Savona, P. B. Littlewood, B. Deveaud, and L. Si Dang, Nature (London) **443**, 409 (2006).

[7]R. Balili, V. Hartwell, D. Snoke, L. Pfeiffer, and K. West, Science **316**, 1007 (2007).

[8]J. J. Baumberg, A. V. Kavokin, S. Christopoulos, A. J. D. Grundy, R. Butté, G. Christmann, D. D. Solnyshkov, G. Malpuech, G. Baldassarri Höger von Hogersthal, E. Feltin, J.-F. Carlin, and N. Grandjean, Phys. Rev. Lett. **101**, 136409 (2008).

[9]V. B. Timofeev, Phys. Usp. **48**, 295 (2005).

[10]L. V. Butov, J. Phys.: Condens. Matter **19**, 295202 (2007).

[11]L. V. Butov, A. L. Ivanov, A. Imamoglu, P. B. Littlewood, A. A. Shashkin, V. T. Dolgopolov, K. L. Campman, and A. C. Gossard, Phys. Rev. Lett. **86**, 5608 (2001).

[12]D. Snoke, Science **298**, 1368 (2002).

[13]Yu. E. Lozovik and V. I. Yudson, Zh. Eksp. Teor. Fiz. Pis'ma Red. **22**, 26 (1975) [JETP Lett. **22**, 26 (1975)]; Zh. Eksp. Teor. Fiz. **71**, 738 (1976) [Sov. Phys. JETP **44**, 389 (1976)]; Solid State Commun. **18**, 628 (1976).

[14]S. I. Shevchenko, Phys. Rev. Lett. **72**, 3242 (1994).

[15]X. Zhu, P. B. Littlewood, M. S. Hybertsen, and T. M. Rice, Phys. Rev. Lett. **74**, 1633 (1995).

[16]O. L. Berman, Y. E. Lozovik, D. W. Snoke, and R. D. Coalson, Phys. Rev. B **70**, 235310 (2004).

[17]V. Larionov, V. B. Timofeev, J. Hvam, and K. Soerensen, Zh. Eksp. Teor. Fiz. **117**, 1255 (2000) V. Larionov, V. B. Timofeev, J. Hvam, and K. Soerensen, [JETP **90**, 1093 (2000)]; A. V. Larionov and V. B. Timofeev, Pis'ma Zh. Eksp. Teor. Fiz. **73**, 342 (2001) [JETP Lett. **73**, 301 (2001)].

[18]D. Snoke, S. Denev, Y. Liu, L. Pfeiffer, and K. West, Nature (London) **418**, 754 (2002).

[19]L. V. Butov, C. W. Lai, A. L. Ivanov, A. C. Gossard, and D. S. Chemla, Nature (London) **417**, 47 (2002); L. V. Butov, A. C. Gossard, and D. S. Chemla, *ibid*. **418**, 751 (2002).

[20]For a review of the spin dynamics of cavity polaritons, see I. A. Shelykh, A. V. Kavokin, Yu. G. Rubo, T. C. H. Liew, and G. Malpuech, Semicond. Sci. Technol. **25**, 013001 (2010).

[21]T. C. H. Liew, I. A. Shelykh, and G. Malpuech, Physica E **43**, 1543 (2011).

[22]N. A. Gippius, I. A. Shelykh, D. D. Solnyshkov, S. S. Gavrilov, Yu. G. Rubo, A. V. Kavokin, S. G. Tikhodeev, and G. Malpuech, Phys. Rev. Lett. **98**, 236401 (2007).

[23]Yu. G. Rubo, A. V. Kavokin, and I. A. Shelykh, Phys. Lett. A **358**, 227 (2006).

[24]O. Kyriienko and I. A. Shelykh, Phys. Rev. B **84**, 125313 (2011).

[25]Yu. G. Rubo and A. V. Kavokin, Phys. Rev. B **84**, 045309 (2011).

[26]A. A. High, A. T. Hammack, J. R. Leonard, S. Yang, L. V. Butov, T. Ostatnicky, A. V. Kavokin, and A. C. Gossard, arXiv:1103.0321.

[27]M. Z. Maialle, E. A. de Andrada e Silva, and L. J. Sham, Phys. Rev. B **47**, 15776 (1993).

[28]R. Winkler, in *Spin-Orbit Coupling Effects in Two-Dimensional Electron and Hole Systems*, Springer Tracts in Modern Physics, Vol. 191 (Springer, Berlin, 2003).

[29]R. H. Silsbee, J. Phys.: Condens. Matter **16**, R179 (2004).

[30]M. Combescot, O. Betbeder-Matibet, and F. Dubin, Phys. Rep. **463**, 215 (2008).

[31]M. Combescot, O. Betbeder-Matibet, and R. Combescot, Phys. Rev. B **75**, 174305 (2007).

[32]S. B. de-Leon and B. Laikhtman, Phys. Rev. B **63**, 125306 (2001).

[33]S. de-Leon and B. Laikhtman, Phys. Rev. B **61**, 2874 (2000).

[34]E. M. Lifshitz and L. P. Pitaevskii, *Statistical Physics* (Pergamon, New York, 1980), Pt. 2.

[35]C. Wu, I. Mondragon-Shem, and X.-F. Zhou, Chin. Phys. Lett. **28**, 097102 (2011).

[36]I. A. Shelykh, Y. G. Rubo, G. Malpuech, D. D. Solnyshkov, and A. Kavokin, Phys. Rev. Lett. **97**, 066402 (2006).

[37]A. A. High, J. R. Leonard, A. T. Hammack, M. M. Fogler, L. V. Butov, A. V. Kavokin, K. L. Campman, and A. C. Gossard, Nature (London) **483**, 584 (2012).

[38]N. W. Sinclair, J. K. Wuenschell, Z. Voros, B. Nelson, D. W. Snoke, M. H. Szymanska, A. Chin, J. Keeling, L. N. Pfeiffer, and K. W. West, Phys. Rev. B **83**, 245304 (2011).

[39]E. Ya. Sherman, A. Najmaie, and J. E. Sipe, Appl. Phys. Lett. **86**, 122103 (2005).

[40]S. Giglberger *et al*., Phys. Rev. B **75**, 035327 (2007).

[41]C. Ciuti, V. Savona, C. Piermarocchi, A. Quattropani, and P. Schwendimann, Phys. Rev. B **58**, 7926 (1998).